Soils and Foundations 2014;54(4):588–607

HOSTED BY

ELSEVIER

CrossMark

The Japanese Geotechnical Society

Soils and Foundations

www.sciencedirect.com
journal homepage: www.elsevier.com/locate/sandf

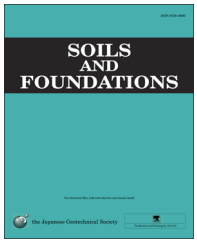

Damage to agricultural facilities

Yoshiyuki Mohri*, Susumu Masukawa, Toshikazu Hori, Mitsuru Ariyoshi

Department of Facilities and Geotechnical Engineering, National Institute for Rural Engineering, Japan

Received 1 April 2012; received in revised form 16 February 2014; accepted 26 March 2014
Available online 10 August 2014

Abstract

The 2011 off the Pacific Coast of Tohoku Earthquake severely damaged agricultural facilities in Tohoku district, damaged coastal dikes and farmland behind the embankment, and disrupted lifelines, such as irrigation systems, in districts far from the coastline.

This report introduces an outline of the damaged agricultural facilities on the basis of the investigations made during inspection visits to those facilities by National Institute for Rural Engineering (NIRE). In Fukushima Prefecture, many small earth dams, other dams, and pipelines were damaged. Among a total of 3730 dams and small earth dams in Fukushima Prefecture, 745 small earth dams were damaged by sliding failure or settlement of embankment. Small earth dams at 3 locations were breached, inflicting severe damage on the regions downstream.

The embankments of two dams for agricultural use, the Nishigo dam and the Hatori dam, located in the Tohoku region, were damaged. In parts of Fukushima Prefecture where trunk pipelines for agricultural use have a total length of 17.8 km, at 7 places pipelines were either exposed or experienced leakages, and severe deformation which did not satisfy standard values was noted at 149 locations.

This paper reports the state of damage typical to each type of facility and the restoration measures that were undertaken.

Keywords: Small earth dam; Pipeline; Earthquake; Failure; Liquefaction; Site investigation; Restoration

1. Introduction

The 2011 Off the Pacific Coast of Tohoku Earthquake caused extensive damage such as the floating and ejection of buried structures as well as the failure of some small earth dams. Mohri et al. 1995 performed a detailed survey on the state of a main agricultural pipeline that broke during the 1993 Hokkaido Nansei-Oki Earthquake, and found that the damage was focused on the ancillary structure. Koseki and Matsuo (1997), Yasuda et al. (1995), and Yamaguchi et al. (2012a) described the ground liquefaction mechanism that caused manholes and pipelines to float up to the ground surface.

In Japan, while there have been no reports of the severe failure of large dams constructed with earthquake resistant design, Yamaguchi et al. (2012b) reported on the seismic behavior of embankment dams during an earthquake. Regarding small earth dams, Hasegawa and Murakami (1996) and Tani (1996) described the damage features and mechanism of the 1995 Hyogo-ken Nanbu Earthquake. Large earthquakes have resulted in the damage of a huge number of small earth dams. For example, the 1995 Hyogo-ken Nanbu Earthquake resulted in damage to 1222 of the 51,000 small earth dams in Hyogo Prefecture, and the 1983 Japan Sea Chubu Earthquake resulted in damage at 1300 locations at small earth dams in Akita Prefecture and Aomori Prefecture. All of these small earth dams damaged by earthquake were constructed before the enactment of the seismic design standard (Ministry of Agriculture, Forestry and Fisheries, 2009), while other small

*Corresponding author.
E-mail address: ymohri@affrc.go.jp (Y. Mohri).
Peer review under responsibility of The Japanese Geotechnical Society.

http://dx.doi.org/10.1016/j.sandf.2014.06.025

dams constructed in accordance with the seismic design standard have been safe. However, it is not clear enough how safe they actually are from a hypothetical earthquake like a Level 2 earthquake.

The 2011 off the Pacific Coast of Tohoku Earthquake breached 0.1% of small earth dams in Fukushima Prefecture, showing that almost all of the small earth dams remained in sound condition. This paper reports on the state of the damaged earth dams and pipelines.

2. Earthquake ground motion in Sukagawa City, Fukushima

The Kumado river region is located in the west part of Sukagawa City in Fukushima Prefecture, as shown in Figs. 1 and 4. A large-diameter pipeline is installed underground, as roughly shown in Fig. 2, in soil comprised of sandy silt with an N value (Standard Penetration Test, SPT) of 10 or less at a depth of about 10 m below the ground surface, and coarse/medium sand with an N value of more than 20 at a depth of about 10 m and deeper. In the hilly and mountainous areas, the ground at the installation depth of the pipeline consists of mainly silt and clay with an N value of 5–10.

Data on the earthquake ground motions of the 2011 off the Pacific Coast of Tohoku Earthquake is shown in Fig. 3: EW acceleration at the K-Net Sukagawa site(FKS017) recorded at Sukagawa City in Fukushima Prefecture. The maximum acceleration of the EW motion was 492.9 cm/s^2. The duration of this motion at the Sukagawa site over 50 cm/s^2 continued for 100 s despite being more than 200 km from the epicenter, which was an earthquake motion never which had been experienced. The distribution of the duration of acceleration over 50 cm/s^2 was located from the Tohoku region to Kanto region (Sasaki et al., 2012). The duration times in the Tohoku region were greater than in the Kanto region. The very long duration time of the main shock resulted in the significant deformation of the ground and soil structure, and induced severe liquefaction of soil (Yasuda et al., 2012). A detailed investigation of the river embankments throughout the Tohoku

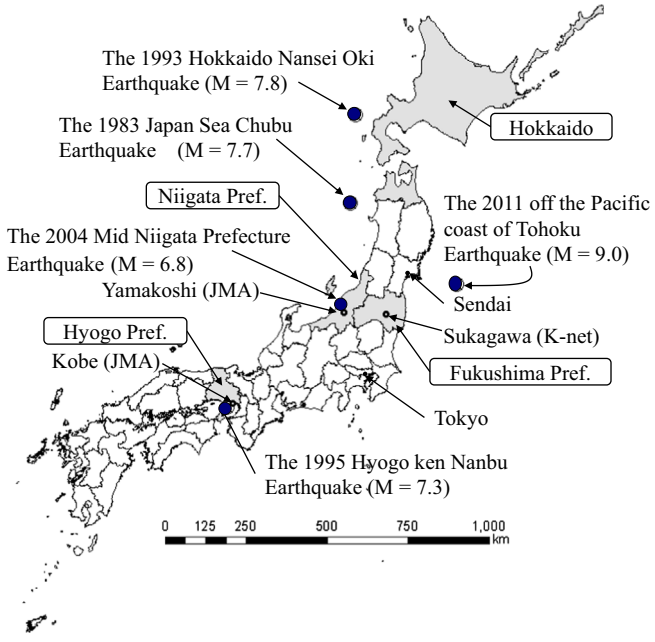

Fig. 1. Locations of earthquake epicenter and investigations.

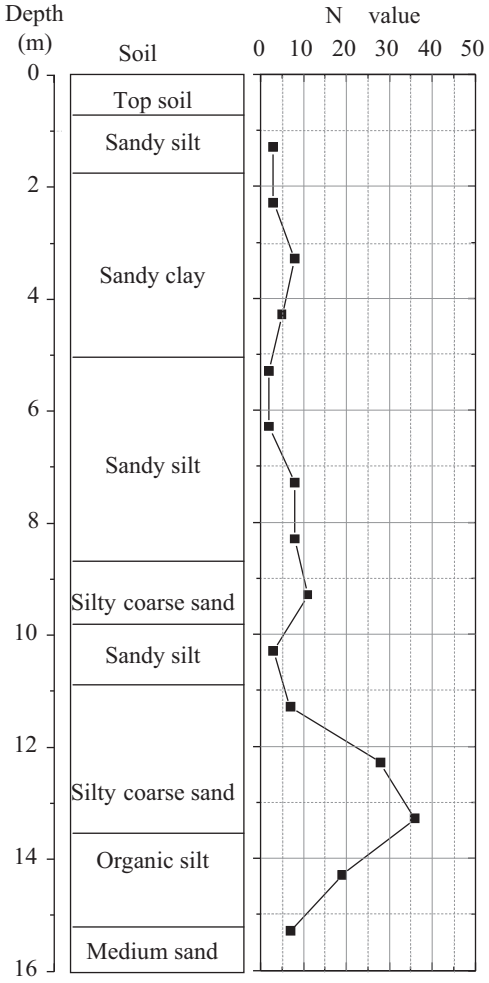

Fig. 2. Result from boring survey conducted before earthquake at Kumado region in Fukushima Pref. (at Ooikenishi Conbined Junction in Fig. 4).

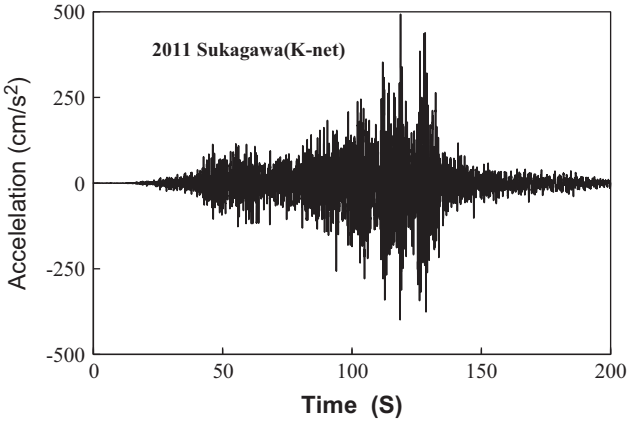

Fig. 3. Accelelation records at Sukagawa (K-net).

and Kanto region was conducted by Oka et al. (2012) and Sasaki et al. (2012), and the results showed that the main causes of damage were (1) liquefaction of the foundations and the river embankments, and (2) the long duration of earthquake. Both the acceleration and the duration time induced the severe damage of soil structures. Such strong motion over such a long duration produced high excess pore water pressure and more deformation of small earth dams and back fill sand of buried pipelines, and resulted in the slip failure of small earth dams and caused buried pipelines to float to the surface.

3. Damage to pipelines

The main agricultural pipeline in the Kumado river region was completed by March 2009. After coming into use in 2010, the pipelines supplied all the irrigation water. The main pipeline, as shown in Fig. 4, starts at the Hiwada diversion work at the intake from the Kumado River and covers a distance of 17.8 km before it reaches Sukagawa City (Ariyoshi et al., 2012). The pipeline system consists of mainly Fiber Reinforced Plastic Mortar pipes (FRPM) ranging from Φ1500 mm to Φ2600 mm in diameter, but steel pipes and ductile iron pipes are also used in some sections. No serious damage was done to the pipes.

In areas with a high groundwater level, the liquefaction of backfill material caused the buried pipes to float up of 1.4 m because of buoyancy, while heavy concrete structures sank as much as 50 cm. The ejection of a joint section of pipe around the structure caused considerable damage, including a large amount of water leakage and surrounding soil washout. For these reasons, not only partial repairs but also pipe replacement and the change of backfill materials was required to resume the water supply through the main pipeline. The pipeline itself, with crushed gravel as backfill, suffered no significant damage or deformation, and showed its earthquake resistance.

3.1. Outline of damaged pipelines

The entire main pipeline in this region, which was filled with water, was affected by the ground motion. According to the design, the allowable internal water pressure for irrigation was 0.35 MPa. Superficial damage to the pipeline included leakage, road settlement and liquefaction of back fill sand of buried pipe. In addition, a detailed investigation into the inner pipes showed nine points with leakage, three points with potential leakage, three points with large settlement and bumps around the valve chambers, three points with settlement of the road crossing the pipeline, and three points with cracks in the road used for pipeline maintenance. This type of damage occurred largely as a result of the liquefaction of the backfill sand, which reduced the bearing capacity of the pipe structure and caused the structure to move, float or settle out of position, leading to the separation of the pipe joints.

3.2. Damage to individual facilities

Pipeline around Ohya No. 7 manhole(air valve works construction completed in 2008)

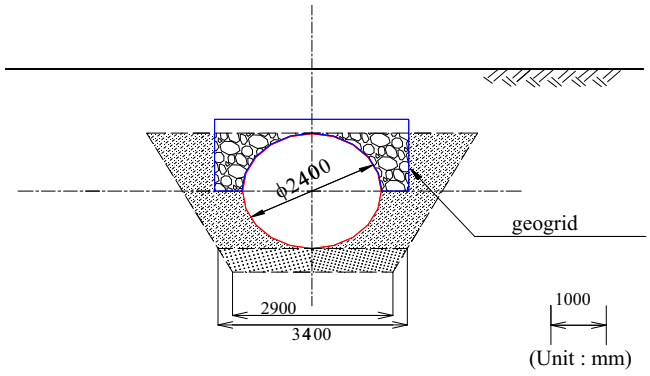

Fig. 5. Cross section for shallow depth of the cover construction method.

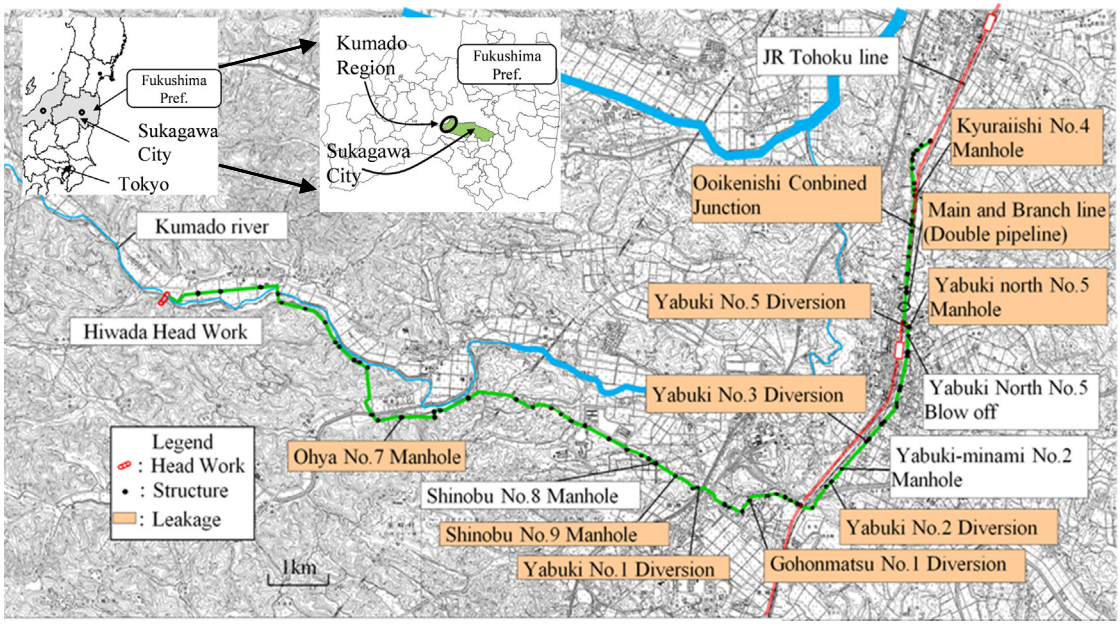

Fig. 4. Plan view of Kumado river irrigation project in Sukagawa City (main pipeline).

A Φ2400 mm FRPM pipe was used for pipes around the manhole. The mean depth of the earth covering for the pipes was specified as about 1.6 m or more, but because the shallow-cover construction method was used, which employs crushed gravel and a geogrid, the actual depth was about 70% of their diameter. When the pipe was installed at a shallow depth, as shown in Fig. 5, crushed gravel around the pipe was wrapped with a geogrid for reinforcement. The backfill material above the center line of the pipe side was crushed gravel (C-30) with a *D* value (degree of compaction) of 92% or more against the maximum standard proctor density. Also, the pipes in this section did not float and they had maintained a designed elevation and joint spacing with no obstruction to the water flow. Consequently, it was estimated that they had stably ensured a water-sealing performance.

3.3. Pipeline around Gohonmatsu No. 1 diversion structure (construction completed in 2009)

A Φ2000 mm FRPM pipe was adopted for pipes around the diversion structure. Crushed gravel, and sand equivalent to SF, was backfilled to the lower and upper parts of the center line of the pipe, respectively. The pipe was installed underground with a depth of earth cover of 2.5 m. One bend pipe with bending angle of 60 was connected another bend pipe with bending angle of 49 between the three FRPM pipes (4-m pipe) and two short pipes (2-m pipe). First bend pipe was connected to the diversion structure. Furthermore, a shaped pipe reducer, which connected the Φ2000 mm pipe to the Φ2400 mm pipe, was installed at a distance of 18 m from the diversion.

As shown in Fig. 6 and Photo 1, the soft ground foundation for the diversion works was replaced with crushed gravel to improve the bearing capacity. For this reason, the embankment of the structure settled only 100 mm deeper than the design elevation, but extensive settlement of the surrounding ground created a bump of 500 mm between the diversion structure and the ground surface. Sand boiled by liquefaction was widely deposited on the surface of the surrounding ground. The upstream and downstream pipes connected to the structure settled 206 mm and 353 mm, respectively. The joints for the upstream and downstream pipes were ejected 360 mm and 465 mm at the crown of the pipes, respectively. The fact that the manholes and pipes generally settled suggests that the settlement of the ground at depths below the pipes was extensive, and the liquefaction of the backfill sand resulted in the considerable deformation of the pipes, causing them to be easily ejected and resulting in the fracture of the pipeline.

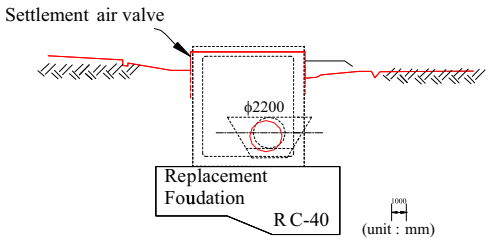

Fig. 6. Cross section for Gohonmatsu diversion.

Photo 1. Settlement of ground around diversion .

Photo 2. Joint ejection at reducer .

The pipes were slightly deflected, with a horizontal deflection rate of about 0.6% (against diameter).

The specially shaped pipe (a steel reducer connecting between Φ2000 mm and Φ2400 mm diameter pipes) that was installed close to this diversion structure was completely displaced. Due to its gradually tapered diameter, it received an unbalanced load (thrust load) in the pipe-axial direction equivalent to the difference of the diameters of the two pipes it connected, under the action of internal water pressure. During the earthquake, it was estimated that a maximum internal pressure of 0.3 MPa acted on the pipes. As a result, a force of about 406 kN was applied to the reducer. The reducer moved 435 mm toward the Φ2000 mm pipe, and was completely ejected, as shown in Photo 2. Leakage from the internal pipe resulted in soil flow, causing a large amount of settlement, which accounted for an area of approximately 10×10 m^2. The ditch on the ground surface in which the pipes were buried settled into grooves, causing axial cracking along the boundary between the backfill and original ground. The ground had

Photo 3. Open crack and settlement of the road above pipeline .

Photo 4. Settlement of ground around manhole .

crack widths of 90 mm and a bump height of 900 mm. The reducer settled 463 mm, and 35 pipes or more (a total length of 140 m) in front of and behind the reducer subsided 200 mm or more. Their horizontal deflections were relatively large, and its deflection rate reached 3.5%, which exceeded the design deflection rate (3.0% of their diameter).

3.4. Pipeline around Yabuki minami No. 2 manhole

For the pipeline section at Yabuki-minami, a Φ2200 mm FRPM pipe was installed underground with a depth of earth cover of about 2.4 m. The pipe was backfilled with sand equivalent to SF from the bottom to the crown level. The density of sand backfill had a D value of 86.9–90.1% or more, which indicates a relatively loose foundation.

The road under which the pipeline was installed had a large open crack 50 cm in width, and had settled over the 1.4 km line, as shown in Photo 3. According to the measurement, the cracking in the road surface reached a depth of 1.6 m, while there was a bump of up to 700 mm between the road and surrounding ground. The cracking of the road surface occurred at the center of the pipe (road), and the shoulders on the right and left banks became lower than the center. This is attributed to the fact that the pipe floated and the embankment slope failed, causing a landslide. As shown in Photos 4, a 1.5 m bump occurred between the Yabuki minami No. 2 air valve structure and the ground, and signs of sand boiling were observed at the boundary between the structure and the

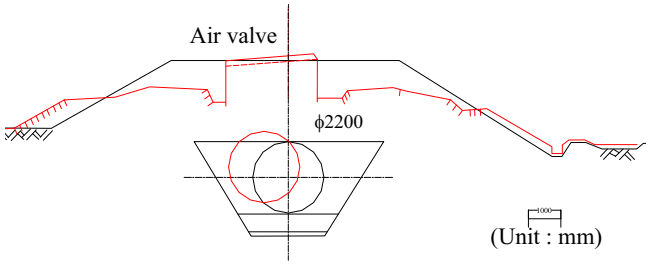

Fig. 7. Cross section for Yabuki-minami district (red line is after earthquake).

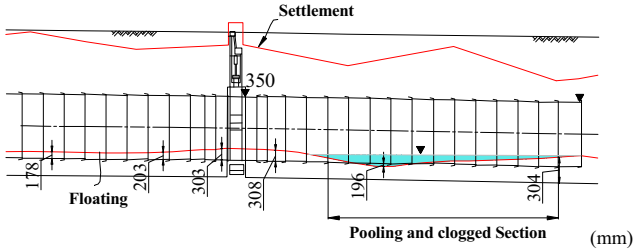

Fig. 8. Settlement of pipeline around manhole, Yabuki-minami (red line is after earthquake).

ground. The cause of the floating pipe is attributed to the liquefaction of the backfill soil, but no large-scale sand boiling was observed on the road surface. As shown in Fig. 7, the road for pipeline maintenance was constructed above the pipe under the embankment design, ensuring the given overburden. However, the road has complicated crossing structures, such as in close proximity to the embankment for the JR Tohoku Line (JR's fill is 5 m from the toe of the slope on the right bank). The JR embankment also meandered and subsided, resulting in a stoppage of train operations. A landslide occurred on the part of the slope in the left bank. It was suggested from this behavior that the liquefaction of the backfill sand for the pipe induced settlement and the landslide of the embankment above the pipe.

The pipes connected to the air valve structure, shown in Fig. 8, were greatly deformed. The pipe at the joint was ejected 350 mm, while the pipes connected to the upstream and downstream sides of the structure settled 363 mm and 338 mm, respectively. Pipes with a total length of at least 130 m floated more than 100 mm. The horizontal deflection of the pipe was measured at five representative points. The results showed that its deflection was 16 (deflection rate of 0.7%) to 65 mm (2.9%).

3.5. Restoration methods

3.5.1. Damage conditions

Along the whole 17.8 km of pipeline, three locations completely lost their water-sealing performance. The probability of occurrence of displacement was 0.07% (3/4033). Among the 149 pipes, as shown in Table 1, the deflection and movement at their joints exceeded the specification values. Specifically, there were 40 pipes (40/1584 = 2.5%) that exceeded the allowable deflection rate of 5%, and 109 pipe

Table 1
Damage situations and number of damaged points.

Damage situation	Number of damaged points
Slip out of joint	3
Pipe deflection rate was 5% or more of its diameter. (allowable deflection rate)	40
Joint-to-joint space was the allowable value or more.	109
Joint-to-joint space fell within the allowable value, and the joint leaked in a seal test.	4
Joint space at the joint ring was the allowable value or more.	1
Eccentricity and expansion of a flexible pipe were allowable values or more.	0
Depth of water retained in a pipe due to the pipe's unevenness was 50 mm or more.	77
Ancillary facilities floated or settled.	11
Diversion and blow-off pipes were deformed.	7
Exteriors and pavements around the ancillary facilities were deformed.	9
Road surface above a pipe was deformed.	26

joints (109/1384=7.9%) that had a deflection exceeding the allowable value. This type of serious damage to the pipeline can be attributed to the fact that the bodies of the pipes floated or meandered due to the liquefaction of the backfill sand, which caused the settlement of the structures and local deformation or ejection of the pipes. For example, a pipeline section under a road or a slope that forms the embankment was dragged along with the slope failure. In particular, the road embankment collapsed due to liquefaction of backfill sand for the pipeline that was installed in the bottom of the road foundation. This suggests that it is important not only to select the appropriate backfill materials for the pipeline, but also to take the effect of the backfill on the surrounding structures and slopes into consideration when designing the pipeline.

3.5.2. Restoration strategy

In order to ensure the structural safety of damaged pipelines and maintain their proper hydraulic functions, (1) pipe replacement; (2) repair work by sealing band at joints; and (3) other countermeasures were selected according to the degree of deformation.

In the section of pipeline where the sand equivalent to SF was adopted as the backfill material for the pipes, the grain-size distribution of the sand shows a high risk of liquefaction. This sand is considered incapable of fully mobilizing its resistance to liquefaction, considering the degree of local compaction (a D value of 88–99% when compared with the standard Proctor maximum density). Fig. 9 (Ministry of Agriculture, Forestry and Fisheries 2009) shows the relationship between the liquefaction stress ratio ($\theta=\sigma_d/2\sigma_c$, σ_d: the amplitude of repeated deviator stress, σ_c: consolidation stress) of sand used as backfill material and the degree of compaction of the sand in the pipeline districts that were previously damaged by an earthquake. These types of sand (SC, SM and SF materials) which are specified as quality backfill sand in the Design Standard (Ministry of Agriculture, Forestry and Fisheries, 2009), in case of liquefaction stress ratio of 0.4 or less and D value of 95% or less, are not considered to have sufficient density in order to avoid liquefaction for severe earthquake like as the 2011 off the Pacific Coast of Tohoku Earthquake. Since the backfill sand in the relevant district has a

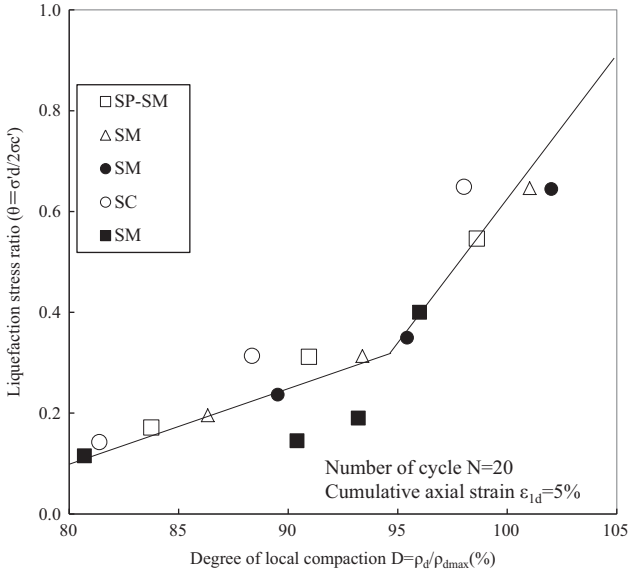

Fig. 9. Liquefaction resistance of backfill sand.

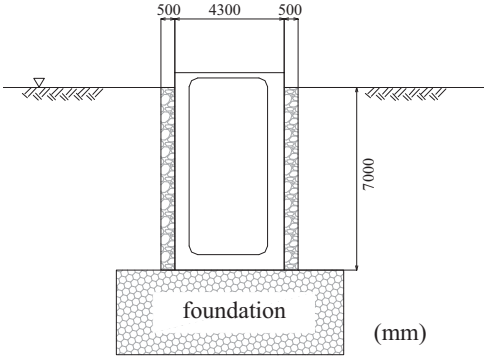

Fig. 10. Cross section for manhole restoration.

D value of about 90%, the liquefaction stress ratio of the sand is estimated to have been about 0.2–0.3. Based on the above discussions, it was decided that crushed gravel is the most suitable for use as backfill in order to improve the resistance to liquefaction in restoring the damaged pipeline sections. Also, in facilities with settlement or floating of concrete structures,

such as manholes, crushed gravel was installed around the entire structure, as shown in Fig. 10.

The reducer in the Gohonmatsu section was completely ejected because the ground could not fully exert sufficient passive earth pressure against the thrust load on the reducer. However, the following factors must be considered: (1) the backfill sand lost its strength due to the increase in excess pore water pressure, and (2) the dynamic water pressure during the earthquake was loaded on the reducer. It is important to fully ensure the material's strength during an earthquake. Consequently, the method shown in Fig. 11 was adopted. Namely, crushed gravel was used as the backfill material in order to suppress the loss of material strength during an earthquake.

3.5.3. Measures against deformed joint in case of the joint exceeds its allowable value

A pipeline with joints absorbs the ground deformation and vibration of the structure through the expansion and contraction of the joints in order to ensure its safety. For this reason, the construction management criteria (Ministry of Agriculture, Forestry and Fisheries, 2005) specify the joint-to-joint space and the bending angle of joints to provide a safety margin. In principle, it is important that the space and the bending angle must be within these specification values, in order to properly maintain the safety and water tightness of a damaged pipeline during its in-service period (about 40 years). Consequently, even pipelines deformed by these ground motions were estimated to be able to repair so that the pipe deflection and joint-to-joint space, the joint's bending angle, and the pipes' unevenness fall within the specification values, with the aim of recovering their performance to the structural function level immediately after their installation. In Table 2, the damage conditions of the pipelines were classified under these four items, and their restoration methods were summarized.

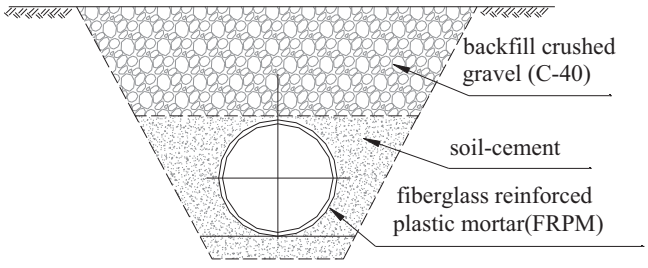

Fig. 11. Backfill around reducer.

(1) For the deflection of a pipe, the allowable deflection (5% of the pipe diameter) that was specified in the Design Standard (Ministry of Agriculture, Forestry and Fisheries, 2009) was used as the reference value.
(2) The control criterion for FRPM pipe joints (FRPM Pipe Association Standard) also applied to the joint-to-joint space for each diameter.
(3) The allowable bending angle specified in the JIS A 5350 also applied to the joint's bending angle.
(4) To deal with unevenness caused by settlement, a construction management reference height of ± 50 mm, which was defined as the specification value in the Civil Construction Management Standard (Ministry of Agriculture, Forestry and Fisheries, 2005), shall be adopted. However, even if a pipeline exceeds this specification value and longitudinally floats or subsides, uniform floating and settlement of the pipeline may cause no damage to its hydraulic functions. For this reason, primary classification of damage levels

Table 2
Damage levels of channels for main pipelines and acceptance criteria for restoration methods.

Level	Damage conditions	Acceptance criteria	Restoration methods
3	A pipe is ruptured, and the joint between pipes is displaced.	There are signs of subsidence, cracking, leakage, etc. of ground surface that resulted from pipe rupture and joint displacement by earthquake, and occurrence of leakage.	
2	Due to lateral deflection of the whole pipe, the pipe loses its required safety level.	(1) An excessive load acts on a pipe due to collapse of upper fill by earthquake, and the deflection rate of the pipe body exceeds the specification value※ (5%).	
	The joint between pipes is deformed.	(2) The joint is deformed by earthquake, and the joint-to-joint space exceeds the specification value [1] or the bending angle exceeds the allowable value.※2	Pipeline replacement
	Displacement of a pipe channel causes projections and depressions to a longitudinal gradient of the pipe, resulting in the loss of blow-off and air exhaustion functions.	(3) Displacement of a pipe channel causes projections and depressions to the longitudinal gradient of the pipe, resulting in the loss of blow-off and air exhaustion functions.	
1	A joint is leaking.	(1) As a result of a water pressure test on the joint, it is confirmed that there is leakage at a point where the joint-to-joint space is the specification value or less and a bending angle is the allowable value or less.	
	A joint is deformed. (applied to an interior tunnel)	(2) The joint is deformed by earthquake, and the joint-to-joint space exceeds the specification value or the bending angle exceeds the allowable value.*The space between the cutting cross section and the pipe in the tunnel is filled with mortar.	Joint repair

*2: allowable bending angle as defined in JIS A 5350.
*1: Civil Construction Management Standards (Rural Development Bureau, Ministry of Agriculture, Forestry and Fisheries).

was be performed as Table 2. Based on the primary classification, the pipeline's hydraulic functions were checked to determine whether or not final restoration was required, and how to rehabilitate the pipeline. Pipeline replacement was made at any point in which sand deposition or air lock may occur that adversely affects its hydraulic functions. The hydraulic functions could not be simply judged due to the heavy dependence on diameter and flow velocity in the pipeline rather than the allowable value of unevenness of main pipelines shall be 50 mm, consistent with the construction management standard for pipes on soft ground. Consequently, an examination was carried out to determine whether or not the unevenness of each pipe could be limited to 50 mm or less to eliminate sand deposition or air lock by the new installation of a blow-off and manhole at a proper point even if the pipeline exceeds the specification value of 50 mm and the whole body of the pipeline floated or subsided significantly.

3.5.4. *Reuse of existing pipes*

Pipes only several years of age were also damaged by this earthquake. For many damaged pipes, their joints were simply ejected, while their bodies were not significantly damaged. For these reasons, FRPM pipes that were pulled out for pipeline replacement meeting the product specifications were reused. Regarding product specifications for FRPM pipes, JIS A 5350 specifies the pipe strength against external and internal pressures and defines the detailed dimensions of their joints. A rubber ring ensures the joints' water-sealing performance, but there is a high possibility that the ring is damaged when a pipe is dug out, while it is difficult to verify the safety of the joints. Consequently, the joint shall be cut off from the body of the pipe in order to reuse the body itself. An additional collar joint shall be connected between the recycled pipes.

The external pressure test was done to determine whether the pipe's rigidity and load bearing performance have deteriorated over time, but only the average performance of its ring piece was tested. For this reason, slight damage to the pipe cannot be verified. Consequently, a test for internal water pressure on the pipe was conducted to check for damage to the interior pipe and damage to the pipe that could not be visually determined, like small pinhole failures.

The results of the external pressure test for the ring piece (ϕ2200 pipe used) did not show any anomalies, such as cracking at 82.1 kN/m (specification value of 63.1 kN/m) during reference deflection (5%, 112 mm) and at a test external pressure (failure load) of 249 kN/m (specification value of 184 kN/m). Under a test water pressure, the strain of the pipe was about 1/4 of the failure strain ($14{,}000–16{,}000 \times 10^{-6}$), while there was no leakage or leaching from pinholes in the pipe body. It was thus determined that these existing pipes had the specified performance. An economical and short-time restoration method was adopted to check the performance of the pipes that were dug out for replacement and to determine if the pipes can be reused: an external pressure test for the ring piece and a water pressure test were conducted.

3.6. *Summary for pipeline*

Not only the periphery of concrete structures, but also the pipes in the linear sections of the pipeline were seriously damaged. There were many damage patterns in which the backfill material was subjected to ground motions and lost its strength, or in which liquefaction floated pipes and subsided structures. A damage pattern was also observed in which the joint between two pipes moved 300 mm or more and the pipes had completely slipped out. It was reported by Fujita and Mohri, 2007 in a study on the damage to agricultural pipelines by past severe earthquakes that the pipes around structures or bend pipes moved a considerable amount during an earthquake and constituted a weak point. In the 2011 off the Pacific Coast

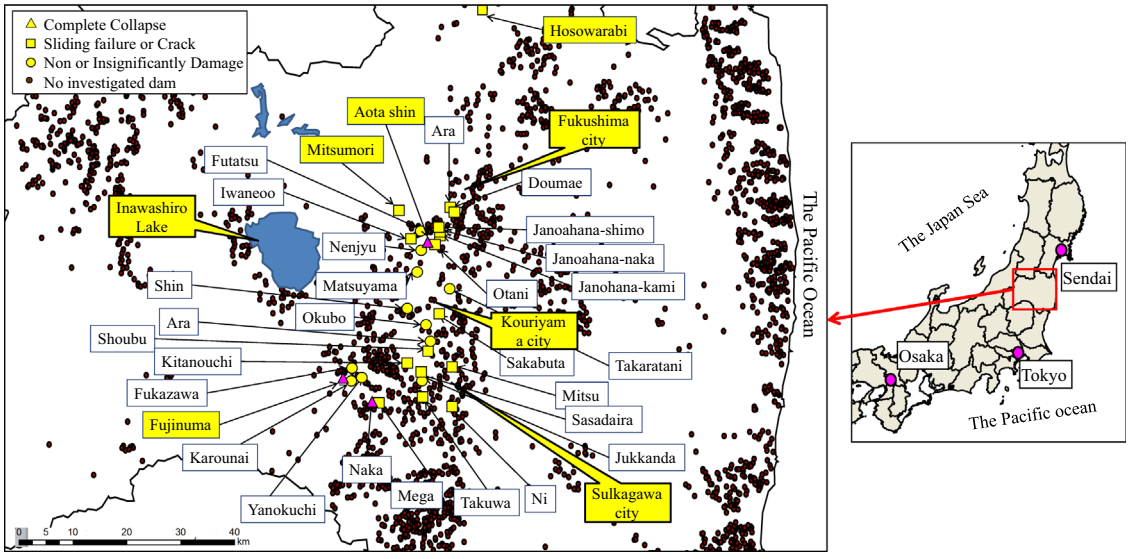

Fig. 12. Locations of investigated small dams and others.

Table 3
Properties of the investigated small earth dams.

Name	Width of crest (m)	Volume (m^3)	Hight (m)	Crest length (m)	Gradient of slope (upstream)	Gradient of slope (downstream)	Reservoir capacity (m^3)	Effective storage capacity (m^3)	Catchment area (km^2)	Full water area (km^2)
Fujinuma	6	9900	18.5	133	2.8	2.5	1,504,000	1,504,000	8.23	0.2
Aota-shin	3	42,220	8.3	275	2.0	2.0	17,000	17,000	0.22	–
Naka	4.5	20,000	11.4	85	2.2	2.0	35,000	35,000	0.24	0.01
Mitsumori	7.5	265,000	28.5	205	2.0	1.4	720,000	720,000	8.2	0.083
Doumae	2	2268	6	84	–	1.4	36,150	24,100	–	0.01
Ara	2.5	7762	9	75	1.2	1.3	48,000	48,000	–	0.023
Iwane-Oho	3	26,730	7.5	26.4	2.0	1.4	59,000	59,000	2.16	–
Ootani	3	14,220	3.8	288	1.4	1.4	59,000	59,000	0.63	–
Jyanohana-nakano	3.5	6850	6.4	153	2.0	2.0	55,000	55,000	0.29	–
Jyanohana-kamino	4.7	7290	5.5	81	–	1.4	24,000	24,000	0.17	–
Ni	5	17,000	8.4	176	2.0	1.8	32,000	32,000	0.18	0.015
Mitsu	2	4700	5	87	1.7	1.7	18,000	18,000	0.63	0.009
Syoubu	7	3800	3.5	105	–	2.0	17,000	17,000	0.1	0.011
Mega	3.5	10,000	6.9	105	2.0	2.0	15,000	15,000	0.36	0.08
Taguwa	3.5	900	3.5	43	2.0	2.2	4000	4000	0.06	0.002
Sasadaira	4	22,400	7.8	180	2.9	2.0	175,700	176,000	0.48	0.052
Futatsu-kami	2	10,630	6.7	127	1.8	1.3	10,000	10,000	1.06	–
Matsuyama	2.5	3100	7	50	1.0	1.5	4500	3800	0.1	0.002
Ara	5.6	5000	5	132	1.4	2.0	25,000	58,000	0.03	0.07
Jitsukanda	4.3	6000	7.5	72	2.0	1.5	38,000	38,000	0.2	0.0106
Karounai	5.2	5200	8	52	1.7	1.4	11,500	3000	0.43	0.004
Yanokuti	3.5	9500	6	120	2.0	2.0	55,000	55,000	0.53	0.025
Toshinaka	2.5	29,540	13	90	1.8	1.8	7350	7000	0.46	–
Jyanohana-simo	3	9030	7	89	1.8	1.3	19,000	19,000	0.29	–

of Tohoku Earthquake, not only structural problems of the pipes such as the pipe bends and configuration of the structures but also the liquefaction of the backfill material significantly affected the main pipelines. On the other hand, pipes with crushed gravel as the backfill material moved only slightly and remained stable.

Furthermore, the remaining performance of the existing pipes was tested to estimate whether or not the pipes could be reused. The pipes that can be reused shall be buried as restoration material. The pipelines that have served only for a short time since the completion of construction have sufficient strength. The reuse of the pipelines led to significant cost reduction and shortening of the restoration period.

4. State of damage to small earth dams

The small earth dams which were investigated can be categorized into three classes for the purpose of reporting on the state of damage to individual small earth dams. They are (1) breached small earth dams, (2) small earth dams which slid or cracked, and (3) small earth dams near damaged small earth dams which were only slightly damaged or were undamaged. Fig. 12 shows their locations and dimension for those small dams are indicated in Table 3. In this figure, the breached small earth dams are indicated by the symbol "Δ", the small earth dams which slid or were cracked by the symbol "□"and the ones which were only slightly damaged or were undamaged are shown by the symbol "○". Small circles indicate the locations of all small earth dams in the region. There are no reports of damage to these small earth dams.

4.1. Breached small earth dams

4.1.1. Fujinuma small dam

The construction of the dam embankment at Fujinuma small dam began in 1937, but after a temporary suspension of work, the dam was completed in 1949. It is an earth dam with maximum section height of 18.5 m, crest length of 133.2 m, and total reservoir capacity of 1,504,000 m^3. From 1977 to 1979, its spillway and parapet were upgraded, from 1984 to 1992, the dam was grouted to prevent leaking and its intake equipment was upgraded. The dam embankment has not been upgraded, since it was embanked long before the enactment of design standards (Ministry of Agriculture, 1956), and the structural design and construction specifications of the dam are those for a small earth dam. The water stored in the Fujinuma reservoir (Fukushima Prefecture, 2011) overflowed and breached the dam because the reservoir, which was full when the earthquake struck, experienced the slide failure of the whole upper embankment from the right to the left abutment during the earthquake (Photo 5). As a result of the breach, severe damage to houses located downstream occurred.

The following points were determined by the excavation exploration of the dam body:

(1) The fill material can be classified into three embankment layers according to differences between the soil quality (top embanking, middle embanking, and bottom embanking), as shown in Fig. 13.
(2) The top embankment layer was 6–8 m thick, its material was generally homogeneous, mostly consisting of gray coarse sand, and there were few clear traces of a compaction layer or spreading.
(3) The middle embankment layer was between 7 and 9 m thick, consisting mainly of brownish gray sandy silt with alternating 20–30 cm layers of sand containing yellowish-gray silt, loam-type clay, and humic silty sand ranging from black to dark gray, and showed clear traces of spreading.
(4) The bottom embankment layer between 4 and 6 m thick, consisted mainly of coarse to fine sand contained gravel including a silt fraction, with alternating 20–30 cm layers of loam type clay and humic silty sand ranging from black to dark gray, and showed clear traces of spreading.

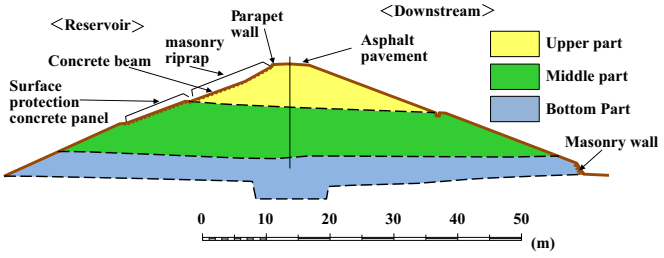

Fig.13. Cross section and classification of embankment layer.

Photo 5. Fujinuma small dam after breach.

The foundation ground is a late quaternary sedimentary layer and a quaternary early diluvium Shirakawa Stratum. The sedimentary layer is distributed under the dam embankment, and its maximum thickness is about 7 m.

In an investigation conducted before the earthquake, it was determined that the average *N*-value of the top embankment was 3, the average *N*-value of the middle and bottom embankment was 4, and no differences were found between the top and middle embankment. Laboratory soil tests of the materials remaining after the earthquake were performed, as shown in Fig. 14 and Table 4.

The mapping of debris of Fujinuma small dam confirmed the following findings.

(1) Most of upper part of embankment was washed away and most of middle and lower part of downstream embankment was also washed away.
(2) From the movement of the structural elements, first masonry riprap of upper part of embankment fell to the reservoir and subsequently the surface protection work from the middle to the right abutment moved substantially to the reservoir (Fig. 15). It was confirmed that slides occurred in the direction both of the reservoir and downstream judging from the distribution of main scarps, sliding surfaces and moved layers.

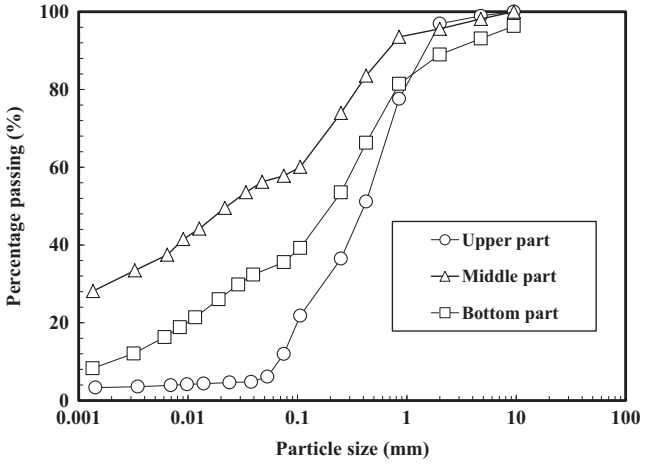

Fig. 14. Particle size distribution of embankment materials.

In the Design Standard (Ministry of Agriculture, Forestry and Fisheries, 2009), the stability of the dam embankment has to be estimated by a circular slip analysis. The safety factor by the criteria based method of stability analysis using the soil strength c' and φ' (Table 4) was 1.15 less than the required value of 1.2 of the criteria when a seismic force of 0.15, which is regulated as a severe earthquake district in the Design Standard (Ministry of Agriculture, Forestry and Fisheries, 2009) is applied to the upstream direction. The cross section for analysis is indicated in Fig. 13.

The investigation revealed that the slides could be broadly classified into seven stages (Fig. 16). Among these slides, the upstream slide Nos.1 and 2 triggered the subsequent overflow and erosion and resulted in the failure of the dam (Fig. 17). The slide failure No.1 occurred in the upper embankment, as was recognized from the remnant of the structural elements in the reservoir, as shown in Fig. 15.

The analysis showed that the quantity of sliding failure towards the upstream side is about 0.81 m in isotropic condition sliding failure, and that cause of the sliding failure was only in the inside of the upper embankment (Tanaka et al., 2012). Earthquake motion for the Modified Newmark Method was estimated by a response analysis using nearest earthquake record from Japan Meteorological Agency data base.

4.1.2. Aota shin small dam

The Aota shin small dam, shown in Fig. 18, is a curved embankment formed by an east side embankment (below, "east dam") and south side embankment (below, "south dam") which was connected at right angles, with its flood spillway constructed on the left bank of the east dam and a bottom conduit installed in the center of the east dam. The dam height is 8.3 m, and the total reservoir capacity is 17,000 m^3, but its repair history is unknown. Residence houses stand directly downstream from the east dam.

The reservoir was full when the earthquake struck, breaching the connection point of the east dam and south dam, discharging all the water in the reservoir (Photo 6). The crest was cracked over its entire surface including the east dam and south dam, and the downstream slope of the east dam (left bank side of the breach) had slide failure. Inundation caused by the breach passed through the houses to flow into downstream paddy fields and small earth dams, but the breach caused no secondary damage to the residential homes.

Table 4
Strength parameters of embankment materials for Fujinuma small dam.

Layer		Facies	*N*-value	Wet density (g/cm^3)	Proctor density (%)	Shear strength	
						c' (kN/m^2)	φ (deg)
Embankment	Upper part	Sandy soil	3	1.70	87.9	14	28
	Middle part	Cohesive soil	4	1.55	81.6–87.4	3	38
	Bottom part	Sandy soil	4	1.75	86.4–93.7	3	40
Foundation	Deposit	Humus soil/gravel	13	1.54	–	18	29
	Weathered fragmental rock	Volcanic deposit	19	1.80	–	–	–

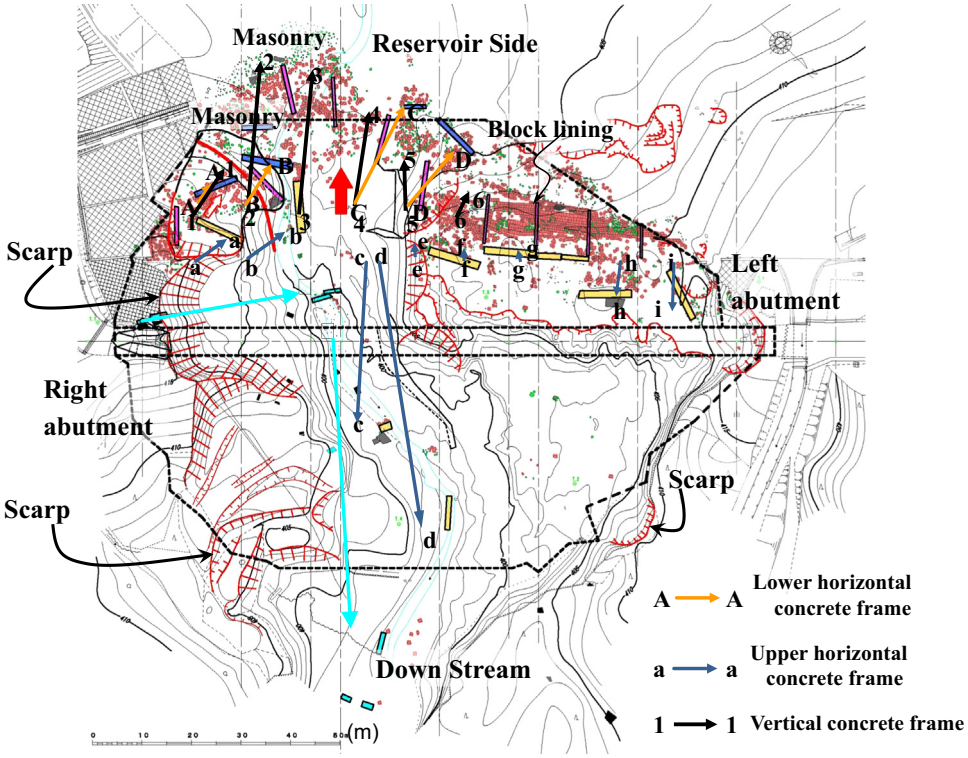

Fig. 15. Mapping of structural elements after failure (quoted from Tanaka, 2012). *Notes*: The dot colored blue is the parapet wall. The dot colored green is masonry riprap. The small square colored purple is the surface protection work. The rectangular colored yellow is concrete beam on the upper upstream slope. Most structural elements moved to upstream.

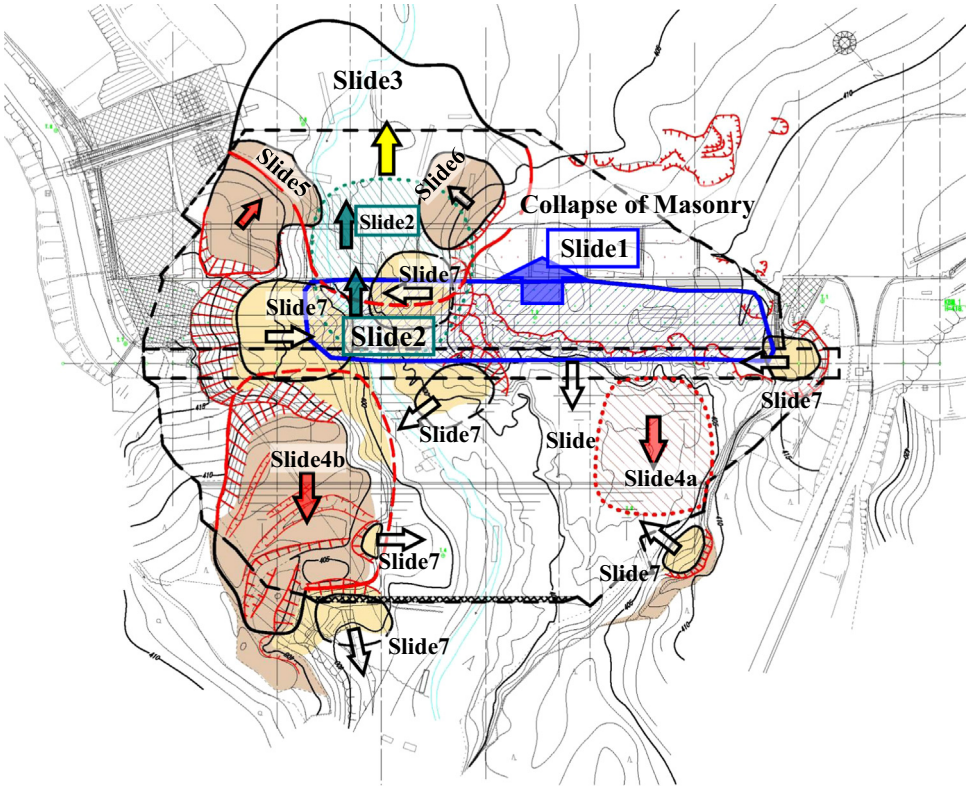

Fig. 16. Integrated map of slides of the Fujinuma main dam (quoted from Tanaka, 2012). *Note*: The solid lines are existing slide bodies. The broken lines are estimated slide bodies which were lost by wash out.

The results of an investigation of the part left after the breach have confirmed that the dam has a uniform soil structure made of clay (Hori et al. 2012). Undisturbed specimens were taken from the remaining part of the dam and provided for triaxial compression test, showing that the strength of the dam soil is $c_d = 40$ kN/m^2, and its internal friction angle $\varphi_d = 28.0$. Examples of the results of using the strength of the dam material obtained by the triaxial compression test to calculate the quantity of deformation by the Newmark Method are shown in Fig. 19. The input earthquake motion used was that recorded at the Koriyama Observation Station observed by K-NET. The analysis has shown that the sliding displacement $\boldsymbol{\delta}$ and the minimum safety factor Fs which were calculated are $\boldsymbol{\delta} = 0.7$ m and Fs = 0.99 respectively under sliding failure of the upstream slope. That is, the settlement of about 0.7 m obtained by the analysis results is not sufficient to explain the failure of the dam.

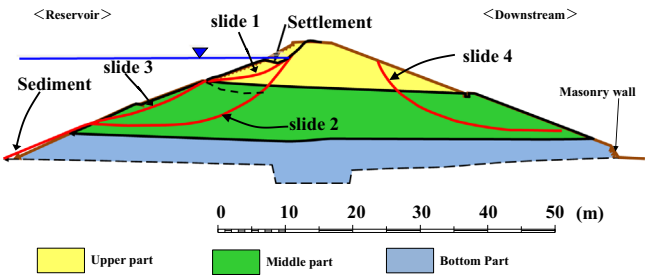

Fig. 17. Following slides after Slide 1.

4.2. Small earth dams which were cracked or slid

4.2.1. Mitsumori small dam

This is a central core zone type dam with height of 28.5 m and total reservoir capacity of 720,000 m^3. In 1939, the dam was completed. In 1955, grouting was carried out between 1980 and 1983 to control leakage, accompanied by other upgrading including raising the dam and improving the spillway, surface protection, and water intake works. The dam was raised by installing a concrete L-shaped retaining wall (vertical parapet) with height of 1.8 m on the upstream slope shoulder, and extra banking of 1.8 m was executed on the dam.

The Mitsumori small dam was full when the earthquake struck, and a longitudinal crack about 130 m long formed on the crest of dam as shown in Photo 7. On the dam on both sides of this longitudinal crack, the upstream side settled lower than the downstream side, forming a step with maximum height of about 60 cm. The concrete vertical parapet on the upstream slope shoulder fell slightly, and this deformation ripped up the masonry directly below the parapet in a scale-like pattern. On the downstream slope about 11 m below the crest, the masonry bulged outwards over the entire dam axis direction (Photo 8). The longitudinal crack on the crest of dam might actually be two cracks. One could have been caused by

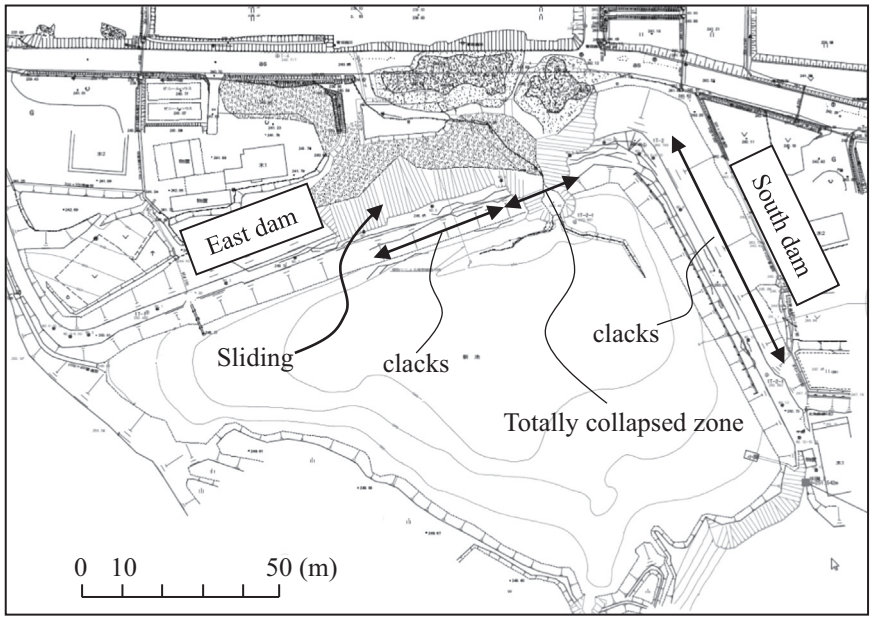

Fig. 18. Plan of Aota-shin small dam after breach.

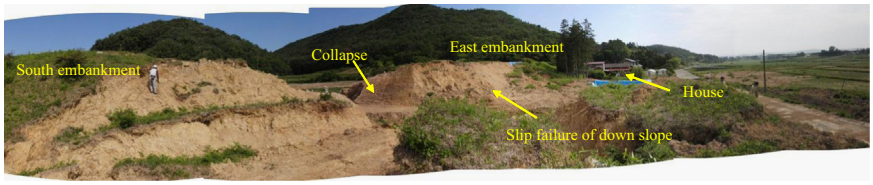

Photo 6. Aota-shin small dam after breach.

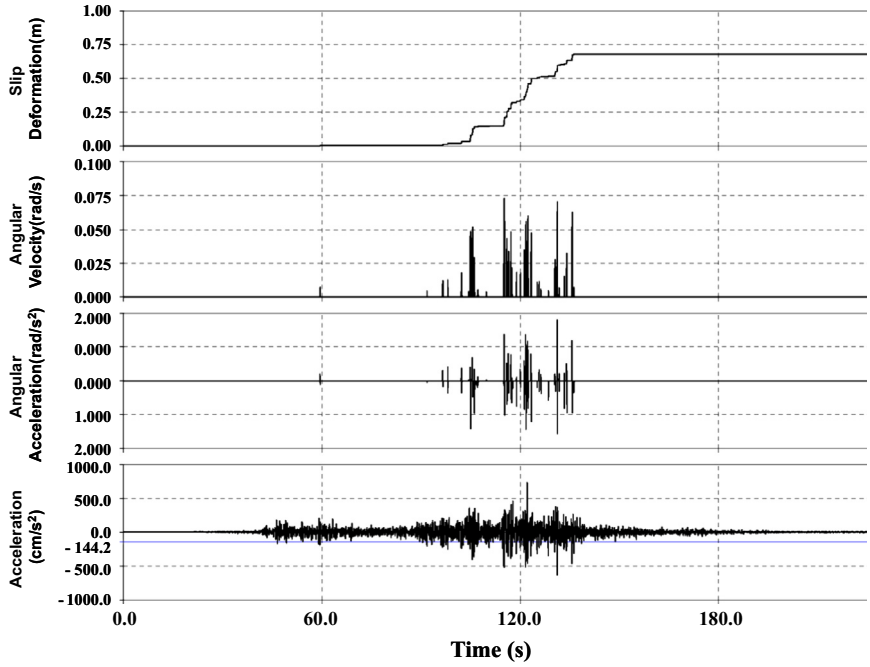

Fig. 19. Calculated deformation of the Aota-shin small dam by the Newmark method.

Photo 7. Longitudinal cracks on the crest of the Mitsumori small dam.

Photo 8. Deformation of stone protection on the upstream slope of the Mitsumori small dam.

the parapet, which was vertically raised, being inclined upstream by the earthquake, causing tension cracking of the extra banking. In this case, the damage was limited to around the extra banking. The second could have been caused by large sliding failure towards the upstream side of the dam. It was feared that aftershocks and the rapid drainage of the reservoir water might induce a sliding failure. In order to confirm the depth and direction of the crack in the crest, slaked lime diluted with water was poured into the crack and, after the crack was colored, a trench was excavated in the cracked part of the dam. The results confirmed that the crack had advanced to a depth of about 4 m in the vertical direction from the crest as shown in Fig. 20. Therefore, it revealed that the deformation of the masonry was limited to the masonry layer being displaced downwards locally by the earthquake, but large sliding failure deformation impacting the entire upstream slope did not occur. It was also confirmed that although the vertical crack reached the impervious core, the damage was almost completely limited to the external banking.

4.3. Classification of damage patterns

The characteristics of earthquake damage to small earth dams is shown in Fig. 21 shows the frequency distribution by damage pattern. The disasters tended to involve multiple damage patterns, so Fig. 21 includes more than one type of damage per site.

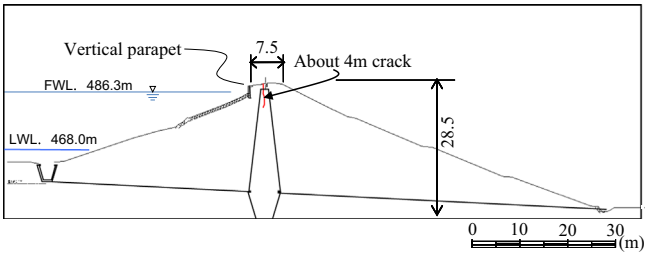

Fig. 20. Cross section of the Mitsumori small dam and depth of the longitudinal crack.

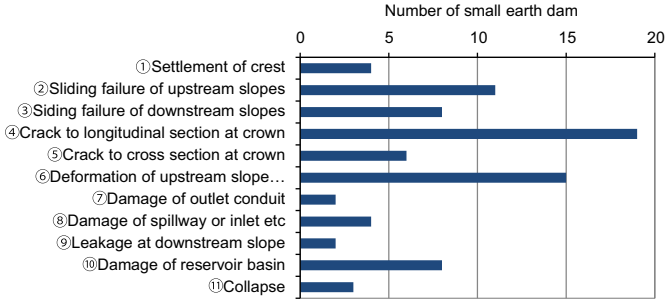

Fig. 21. Affected rate by damaged pattern for small dam.

(1) Settlement of the crest of dam

The settlement of the crest is caused by compression due to shaking or the upstream/downstream movement of the sliding mass.

(2) Sliding failure/bulging of upstream slopes.

This is the second most common type of damage pattern. During an earthquake, cyclical loading reduce the strength of the dam soil, resulting in shear failure on saturated upstream slopes.

(3) Sliding failure of downstream slopes.

In many cases where sliding failure of downstream slopes has occurred, the upstream slope is also deformed, accompanied by settlement of the crest.

(4) Longitudinal cracking section at crest.

This was the most common damage pattern. Longitudinal cracks on the crest can be classified into two types. One type occurs vertically when the dam shakes in the upstream–downstream direction, producing deformation and settlement in the crest. The other is caused by the sliding failure of either the upstream slope or downstream slope.

(5) Transverse cracking at the crest.

Cross-sectional cracks at the crown occur in the downstream–upstream direction of a dam. They often occur on bends in the dam or connections with the natural ground. Continuous cracks in the upstream-downstream direction of a dam are caused by differencial settlement of the dam and natural ground, causing severe leakage.

(6) Deformation of upstream slope protection and the riprap.

A phenomenon characteristic of this disaster is the toppling of the riprap. In the area investigated, where many riprap are protected by either a vertical or steeply inclined concrete retaining wall, many toppled.

4.4. Summary of small earth dams

As seen in past earthquake damage, damage patterns included longitudinal cracks and downstream slope sliding failure on many dam bodies accompanied by sucking out of dam soil as a result of toppling of bulwarks on steep slopes and the breakage of bottom conduits. Only minor damage was noted in the embankment of the Yanokuchi small dam, located just 2.3 km from the Fujinuma small dam, most likely because upgrading, done since about 1993 limited the damage. Therefore, it can be assumed that earthquake resistance performance has been provided to the small earth dams which had been upgraded in recent years by the seismic design method and construction technology.

5. State on damage to dams

The Nishigo dam (dam height = 32.5 m, zone type earthfill dam, active storage capacity = 3,064,000 m^3) was completed by 1955 and the Hatori dam (dam height = 37.1 m, zone type earthfill dam, active storage capacity = 25,951,000 m^3) also was completed by1956. The following are reports on the results of investigations of the the Hatori dam and the Nishigo dam in Fukushima Prefecture, which have been in use over the long term, exceeding half a century.

5.1. The Hatori dam

5.1.1. Outline of the dam

The Hatori dam has the largest surface area of reservoir and the largest amount of storage capacity of all earth dams in Japan. The water storage efficiency of the Hatori dam is very good because it is a small volume dam. A typical cross section of the Hatori dam is shown in Fig. 22. The strength parameters of the embankment material of the Hatori dam were $c = 0.41$ kg/cm2, $\varphi = 8^\circ$ at the upstream side of dam and $c = 0.88$ kg/cm2, $\varphi = 15^\circ$ at the downstream side of dam. A minimum safety factor against sliding by the slip circle method, that is simpler than stability calculation of present design basis, was 1.70 on the upstream slope, and 4.46 on the downstream slope by these strength parameters (Masukawa et al., 2012).

5.1.2. State of damage

The following three types of damage were confirmed after the earthquake. (1) Cracks at construction joints of asphalt pavement used for the prefectural road on the crest of dam. (2) Opening at the joints of the parapets and displacement in the horizontal direction and/or the upstream–downstream direction of the parapet in the both side of the joint. (3) Deformation with a crack directly below the slope shoulder on the downstream of the dam. The quantity of seepage increased after the earthquake, but because it was corresponding to time when the snow melted at the earthquake, it is difficult to conclude that the seepage increased only as a result of the impact of the earthquake. Turbidity of the seepage water was not observed.

The degree of compaction of Zone 1 (impermeability zone) was between 88 and 93%, while the degree of compaction of

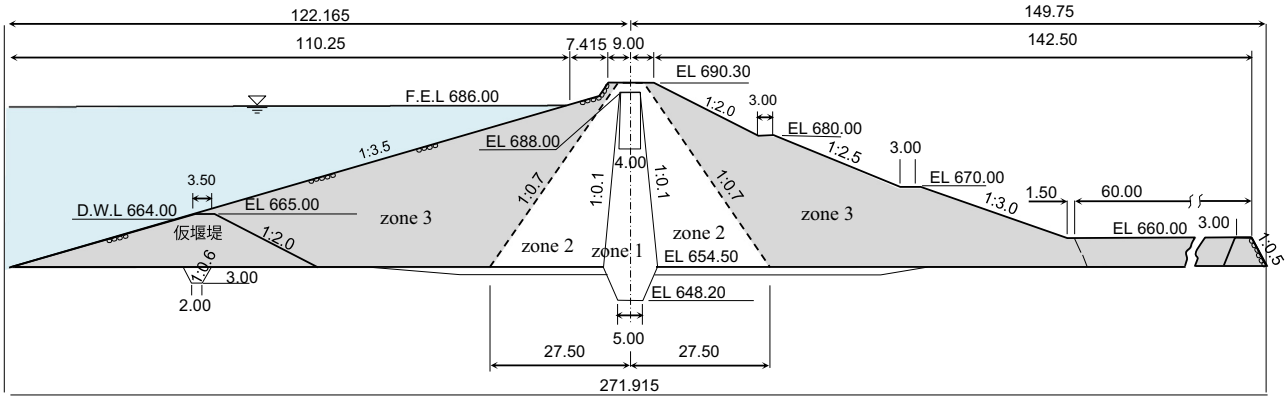

Fig. 22. Typical cross section of the Hatori dam.

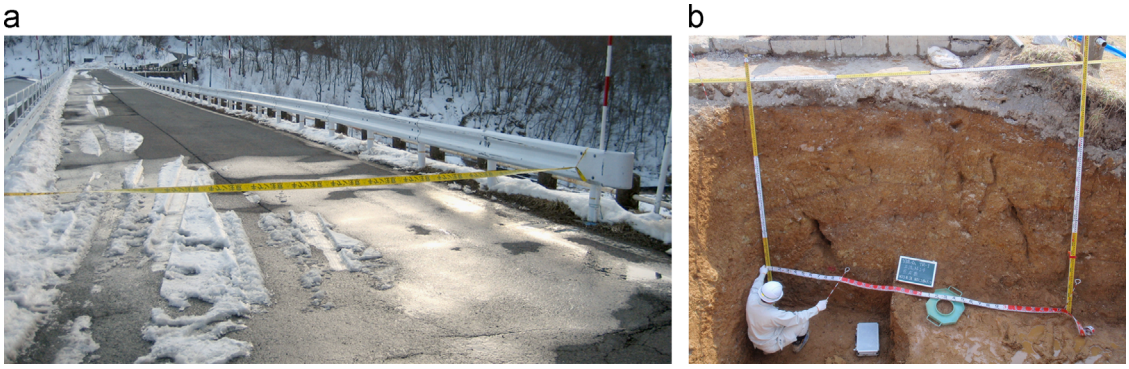

Photo 9. (a) Crack of asphalt pavement road on the crest of the Hatori dam and (b) trench investigation at the cracks on the crest of dam (Tohoku Regional Agricultural Administration Office).

Zone 2 (semi-permeability zone), Zone 2 located at the upstream and downstream sides of Zone 1 and Zone 3 formed the upstream and downstream slope, was 99%, obtained by in-situ density test at an exploration trench and compaction test in a laboratory. The results of the triaxial compression test were $c=20$ kN/m^2 and $\varphi=33^\circ$ for Zone 1, and $c=14$–17 kN/m^2 and $\varphi=34$–35° for Zones 2 and 3.

5.1.3. Crest of dam

On the crest of dam to right abutment from the center part of the crest, there was cracking of the asphalt pavement construction joints located in the centerline of the road on the crest of dam (Photo 9). The maximum opening width of the crack was 53 mm on the right abutment at the crest of dam, and the maximum level difference of the crack that had fallen in the downstream was 21 mm. A 30 mm wide crack on the surface of the embankment material (Zone 2) in the center part of the crest of dam, which was located directly below cracking of asphalt pavement, was confirmed to extend to a depth between 2.45 m and 2.7 m by an exploratory trench. The direction where crack progresses were vertical, but at greater depth, it bent slightly downstream.

In the parapet of the 40 m section at the center part of the crest of dam, settlement up to 79 mm and pushing out to upstream of 78 mm occurred. Parapet connecting blocks were cracked and broken, with maximum crack length of 1 m and 12 mm wide breakage of blocks. On slopes lower in elevation than the connecting blocks of the parapet work (riprap), no deformation such as cracks, breakage, or bulging was confirmed.

5.1.4. Downstream slope

Towards the right abutment from the center part of the crest of dam, open cracks parallel to the dam axis formed on the downstream slope of 2–3 m below the downstream shoulder of the crest of dam. The largest deformation was cracks with width of 120 mm and level differences of 220 mm (r upstream side fall) at the right abutment side of the crest of dam (Photo 10). In the exploratory trench, this crack had a maximum depth of 1.40 m.

5.1.5. Restoration plan for the Hatori dam

The dam embankment above the foundation of the present parapet will be horizontally removed. The width of the crest of dam restored embankment must ensure the specified road width because the crest of the dam is used as a prefectural road. As such, the dam center of the crest will be moved about 5 m in the downstream direction and a surcharge embankment will be constructed on the downstream slope, as indicated in Fig. 23.

5.2. The Nishigo dam

5.2.1. Outline of the dam

A typical cross section of the Nishigo dam is shown in Fig. 24. The stability of the dam was evaluated by the simpler slip circle method as well as the stability calculation of the Hatori dam. A safety factor against sliding at F.W.L. was 2.4 on the upstream slope by $c=0.5$ kg/cm^2 and $\varphi=15^\circ$.

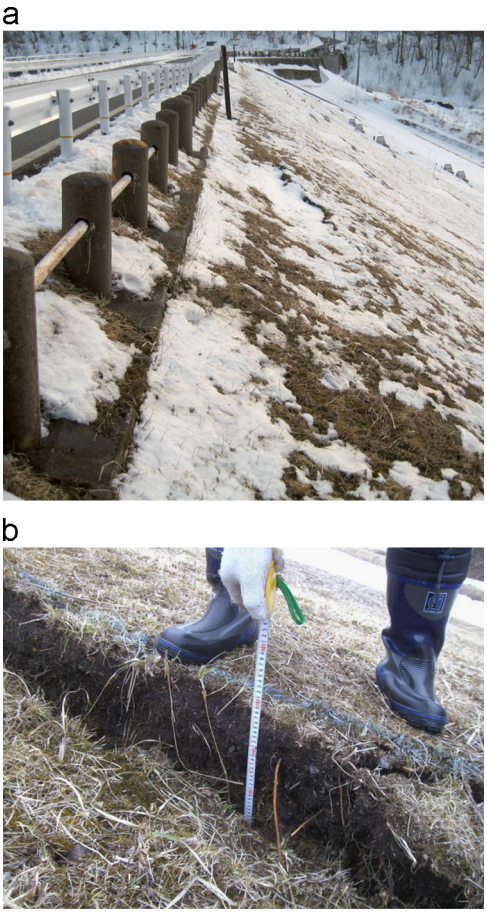

Photo 10. (a) deformation at the top of downstream slope of the Hatori dam and (b) ramp crack on downstream slope (Tohoku Regional Agricultural Administration Office).

5.2.2. State of the damage

The following three kinds of deformation were found on the Nishigo dam. (1) Ramp, subsidence, slipping of riprap, and bending of concrete frames on the upstream slope of the dam, (2) cracks in the dam axis direction on the crest of dam, and (3) settlement of a parapet on the upstream shoulder of the crest of dam and opening and level differences between the dam embankment and the foundation of the parapet. The degree of compaction of the clay, which is the impermeability zone of the dam, was between 80 and 95%, and that of the semi-permeability zone was between 86 and 95%, obtained by an in-situ density test at an exploration trench and a compaction test in a laboratory. The strength parameters of the embankment material obtained by triaxial compression test were $c=17$ kN/m^2 and $\varphi=37^\circ$ for the impermeability zone, $c=14$ kN/m^2 and $\varphi=39^\circ$ for the semi-permeability zone and $c=15$–21 kN/m^2 and $\varphi=36$–38° for the permeable zone.

5.2.3. Upstream slope protection work

A horseshoe-shaped pocket with maximum settlement of 550 mm was formed on the upstream slope below 2 and 3 m from the parapet foundation. This pocket appeared by moving the riprap materials to downwards. A concrete frame installed on the slope below this deformation was bent downwards, the boulders has risen at the concrete frame that was bent (Photo 11). Backfill consisting of small round gravel, which was embanked parallel to the slope, existed under the bottom of the boulders in the three exploratory trench of the upstream slope. An embankment with a thickness of about 1 m, including a continuous softened layer with a high water content, was embanked in parallel to the slope under the backfill. The average degree of compaction of this embankment was about 75%, obtained by an in situ density test at an exploratory trench and a compaction test in a laboratory. The embankment under the approximately 1 m thick embankment was well compacted clay. The cone penetration resistance of this embankment ranged between 1000 and 1500 kN/m^2 in situ, and

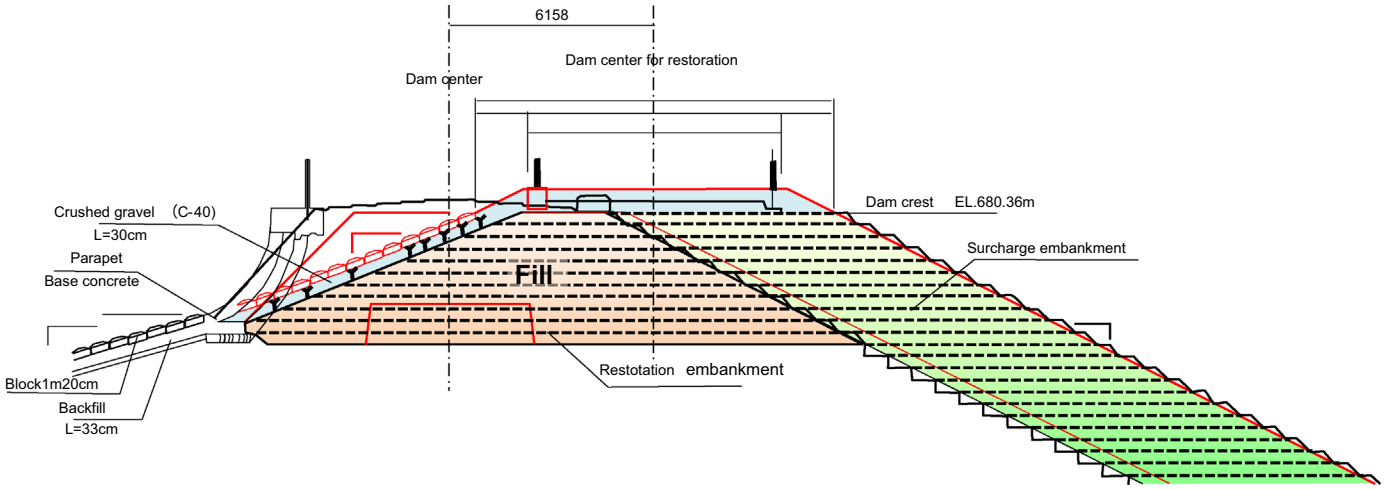

Fig. 23. Section of restoration works at the Hatori dam (constructed in 2011) .

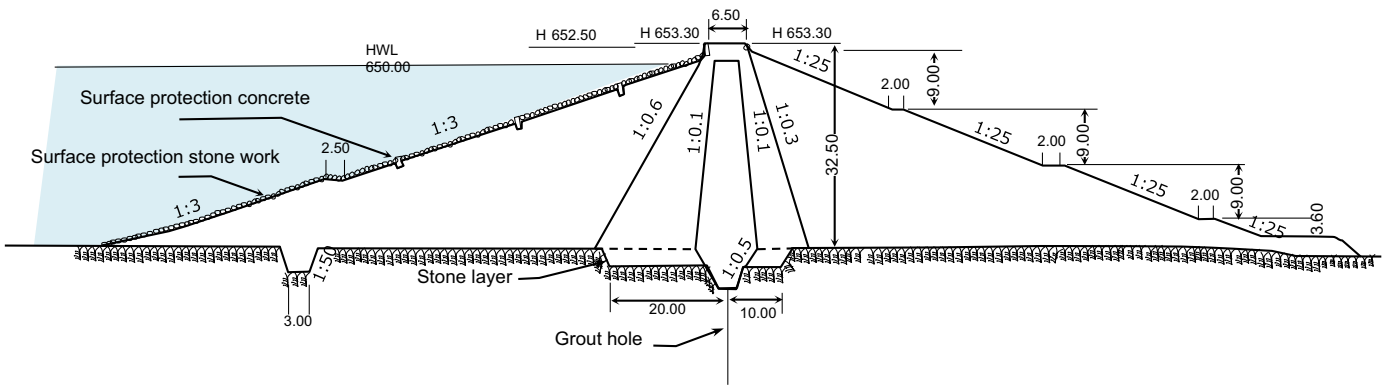

Fig. 24. Typical cross section of the Nishigo dam.

Photo 11. Horseshe-shaped pocket and bending of concrete frame on upstream slope of the Nishigo dam.

Photo 12. Open cracks along dam axis direction on the crest of the Nishigo dam.

the degree of compaction was between 95 and 96% according to the results of the in situ density test at an exploratory trench and a compaction test in a laboratory. This embankment is equivalent to a permeability zone.

5.2.4. Crest of dam

One to three cracks with maximum opening width of 500 mm formed parallel to the dam axis in a section equal to about 2/3 of the dam crest (Photo 12). An exploration trench on the dam crest revealed that the maximum depth of the cracks was 2.75 m, and that although the cracks approached the boundary of the clay and the cover layer, the cracks did not reach the clay (Photo 13). The embanked soil around the cracks was well compacted. Below the ends of the cracks, cone penetration resistance of about 1000 kN/m^2 was obtained.

5.2.5. Parapet work

Settlement and tilting of the concrete parapet works were visually confirmed. At the tops of the parapet works, there was a tendency for settlement up to 360 mm to occur from the design elevation at the center part of the crest of dam. Openings and level differences at the connection of the parapet foundation and upstream slope included maximum openings of 70 mm near the center part of the crest of dam and maximum level difference of 240 mm near the left bank.

5.2.6. Restoration plan for the Nishigo dam

As well as restoration with the Hatori dam, the parapet will be removed and the dam will be horizontally removed to the depth reached by the cracks opened on the crest of dam. The upstream slope will be removed to a depth of 2 m, which is equivalent to the boulders, backfill and embankment constructed in parallel to slope on the entire slope surface. In order to ensure the crest elevation and width, the restoration embanking on the upstream slope will obtain restored embankment gradient of 1:3.0, which is gradient equal to the present slope gradient, but above the design flood water level, it will be 1:2.0. That of the part of the downstream slope which will be removed will be reconstructed to a slope of 1:2.0 (Fig. 25).

Photo 13. Surface of trench sides at open cracks on the crest of the Nishigo dam.

6. Conclusions

Pipelines and small earth dams, other dams incurred a variety of different types of damage in the Tohoku Region. A considerable amount of damage was confirmed on small earth dams, mainly on the main pipeline backfilled by sand and installed in the soft ground foundation, which were not designed and constructed according to modern seismic design. An inspection and repair project performed to clarify the state of deterioration of small earth dams at 210,000 locations was effective, but there is an urgent need to carry out further earthquake resistance countermeasures. It is also essential to identify facilities at other dams which also do not meet present standards related to seismic performance and to complete countermeasures. The following are the results of a damage survey of these investigations.

(1) Embankment dams planned, designed, and constructed at the dawn of the establishment of modern embankment dam design and construction, before the establishment of stability evaluation under the present earthquake load, were not seriously structurally damaged. That is, their water cutoff, storage and discharge functions remained intact.
(2) The most characteristic damage noted in dams and small earth dams was open cracks in the crest of dam along the dam axis.
(3) Among the total of 65,100 small earth dams, 48,500 were constructed before seismic design was established. It is now necessary to perform an earthquake resistance diagnosis of each of these dam bodies and to develop efficient countermeasure technologies.

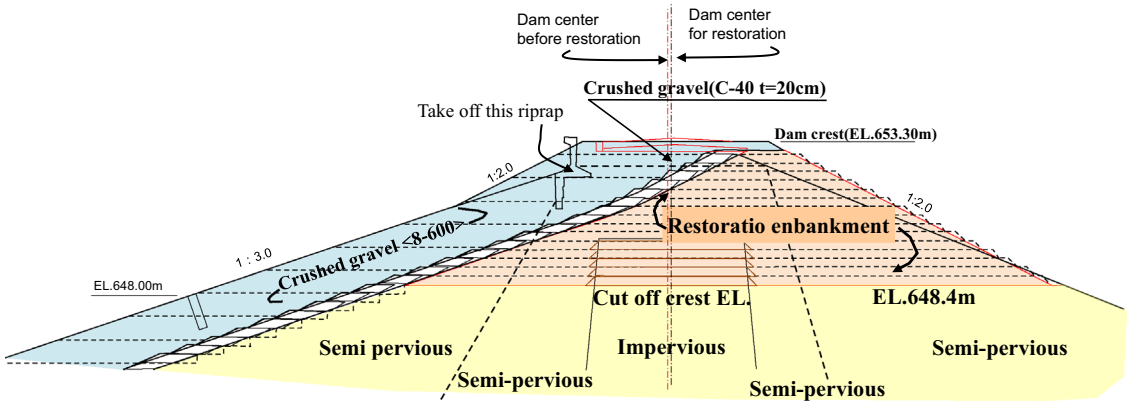

Fig. 25. Section of restoration works at the Nishigo dam (planned in 2011).

The large-diameter pipes received ground motions from seismic intensity of Upper 6. The ancillary concrete structures backfilled by sand, which was concrete manhole and thrust block, were seriously damaged, including the settlement of structure and ejection of joint of surrounding pipes. Pipes with crushed gravel backfill were not damaged because no liquefaction took place in the backfill.

Acknowledgments

This paper is based on the investigation by large number of engineers and researchers involved with Kumado river district project branch in Ministry of agriculture and Fukushima Prefecture, NIRE.

The authors wish to express their sincere gratitude to all for providing the useful information and permission to present data.

References

Mohri, Y., Yasunaka, M., Tani, S., 1995. Damage to buried pipeline due to liquefaction induced performance at the ground by the Hokkaido Nansei-Oki earthquake in 1993. In: Prroceedings of the First International Conference on Earthquake Geothecnical Engineering, IS-Tokyo, pp. 31–36.

Koseki, J., Matsuo, O., 1997. Liquefaction induced uplift of sewer manholes and pipes. In: Proceedings of the 3rd Asian Young Geotechnical Engineers Conference, pp. 549–557.

Yasuda, S., Nagase, H., Itafuji, S., Sawada, H., Mine, K., 1995. A study on the mechanism of the floatation of buried pipes due to liquefaction. Soil Dyn. Earthq. Eng., 125–132.

Yamaguchi, A., Mori, T., Kazama, M., Yoshida, N., 2012a. Liquefaction in Tohoku district during the 2011 off the Pacific Coast of Tohoku earthquake. Soil Found. 52 (5), 811–829.

Yamaguchi, Y., Kondo, M., Kobori, T., 2012b. Safety inspections and seismic behavior of embankment dams during the 2011 off the Pacific Coast of Tohoku earthquake. Soil Found. 52 (5), 945–955.

Tani, S., 1996. Damage to earth dams. Spec. Issue Soil Found., 263–272.

Hasegawa, T., Murakami, A., 1996. Damage to agricultural facilities. Spec. Issue Soil Found., 255–261.

Ministry of Agriculture, Forestry and Fisheries, 2009. Planing and design criteria of land improvement project “Pipeline”. Design code (in Japanese).

Sasaki, Y., Towhata, I., Miyamoto, K., Shirato, M., Narita, A., Sakai, T., Sako, S., 2012. Reconnaissance report on damage in and around river levees caused by the 2011 off the Pacific coast of Tohoku earthquake. Japan. Soil Found. 52 (1), 1016–1032.

Oka, F., Tsai, P., Kimoto, S., Kato, R., 2012. Damage pattern of river embankments due to the 2011 off the pacific Coast of Tohoku earthquake and a numerical modeling of the deformation of river embankments with a clayey subsoil layer. Soil Found. 52 (5), 890–909.

Yasuda, S., Harada, K., Ishikawa, K., Kanemaru, Y., 2012. Characteristics of liquefaction in Tokyo Bay area by the 2011 Great East Japan Earthquake. Soil Found. 52 (5), 769–779.

Ariyoshi, M., Mohri, Y., Asano, I., Ueno, K., 2012. Damage and restoration of agricultural pipeline at Kumadogawa irrigation project by the 2011 off the Pacific coast of Tohoku earthquake. Technical report in NIRE, No.212 (in Japanese).

Ministry of Agriculture, Forestry and Fisheries, 2005. Construction management criteria of land improvement project. Rural Development Bureau (in Japanese).

Fujita, N., Mohri, Y., 2007. Performance of Flexible Joints formed Underground Pipeline – Estimation of Joint Expansion and Verification by Model Test, No. 249(75-3), pp. 293-303 (in Japanese).

Ministry of Agriculture, 1956. Planing and design criteria of land improvement project “Earth dam”. Design Code (in Japanese).

Fukushima Prefecture, 2011. Agriculture and fishries devision. Home Page 2011 ⟨http://wwwcms.pref.fukushima.jp/download/1/230427affhigai-02.pdf⟩.

Tanaka, T., Tatsuoka, F., Mohri, Y., 2012. Earthquake induced faiIure of Fujinuma Dam, ICOLD 2012 KYOTO. In: Proceedings of the International Symposium on Dams for a Changing World, pp. 6.47–6.52.

Hori, T., Ueno, K., Matsushima, K., March, 2012. Damages of Small Earth Dams Induced by the 2011 Earthquake of the Pacific Coast of Tohoku, Technical report in NIRE, No. 212 (in Japanese).

Masukawa, S., Tagashira, H., Kuroda, S., Hayashida, Y., 2012. Damages of Embankment Dams for Irrigation due to the 2011 off the Pacific coast of Tohoku Earthquake, Technical report in NIRE, No. 212 (in Japanese).